Practical Limitations Of Low Field NMR Measurements of ^{13}C and ^{23}Na.

Michael J. Dick[1], *Dragan* Veselinovic[1], *Taylor* Kenney[1] *and Derrick P.* Green[1]

[1]Green Imaging, 520 Brookside Drive, Suite B, Fredericton, NB, Canada

Abstract. Low magnetic field ^{1}H NMR has been employed for decades as a tool in core analysis laboratories. Measurement of other NMR active nuclei have not been as common because these measurements typically require very expensive strong magnetic field instruments with cryogenic cooling. However, in recent years there has been new data showing that NMR measurements of other active nuclei can be beneficial for core analysis. For example, it has been shown that ^{13}C NMR measurements (in conjunction with ^{1}H measurements) can be employed to determine the relative saturation of water and oil in a core sample, help determine wettability and examine CO_2-Brine-Rock interactions for evaluation of carbon capture utilization and storage. Our goal has been to develop a new NMR probe capable of observing both ^{13}C and ^{23}Na at lower field. This new $^{13}C/^{23}Na$ probe was designed to work in our existing 0.3 Tesla magnet. This meant that one magnet can be employed to measure both hydrogen, sodium and carbon NMR data by simply swapping out the ^{1}H probe (Larmor Freq. – 12MHz) for the $^{13}C/^{23}Na$ probe (^{13}C-Larmor Freq. – 3.25 MHz and ^{23}Na-Larmor Freq. – 3.41 MHz). While ^{1}H and ^{23}Na have a natural abundance of 100%, ^{13}C has a natural abundance of only 1%. This leads to a lower signal-to-noise ratio (SNR) for the ^{13}C data leading to longer scan times as compared to ^{1}H. In addition, employing lower magnetic fields for ^{13}C and ^{23}Na further reduces the NMR signal leading to even lower SNR further lengthening scan times. Another experimental challenge that had to be overcome in development of the $^{13}C/^{23}Na$ probe was the fact that working at a lower field made the probe more susceptible to acoustic ringing. A lot of effort was spent exploring how different copper shielding configurations and different materials employed for the probe body could reduce the acoustic ringing. Despite all these challenges, the new $^{13}C/^{23}Na$ probe was successfully completed and commissioned. Eventually, T_2 and T_1 distributions, one dimensional saturation profiles and T_1-T_2 maps were acquired for ^{13}C of different bulk samples including glycerol, decane and crude oil. For ^{23}Na, brines with differing sodium concentrations (2-25%) were measured both in bulk and in saturated core samples. Finally, both the ^{23}Na and ^{13}C T_2 measurements were employed in conjunction with and ^{1}H T_2 measurements to derive the relative saturation of water and oil in different samples.

* Corresponding author: author@e-mail.org

1 Introduction

Nuclear Magnetic Resonance (NMR) core analysis has become a fixture in core analysis labs around the world. Traditionally, ^{1}H is the nuclei of choice for core analysis. ^{1}H is NMR active and has a high natural abundance making it easy to observe. In addition, ^{1}H is also present in both fluids commonly present in core samples (oil and water). For both these reasons, ^{1}H based NMR measurements are well suited to core analysis experiments. Three types of ^{1}H NMR measurements are typical in NMR core analysis experiments. Firstly, the amount of hydrogen in a core sample can be determined non-destructively. NMR measurements are an excellent way of determining the porosity of core samples. Secondly, the NMR measurement can localize the hydrogen in a core sample. This means one-dimensional (1D), 2D, or 3D images locating the oil or water in a core sample can be created from NMR data. Finally, NMR signal lifetimes depend on the environment that the hydrogen within the core experiences. It is this correlation between environment and signal lifetimes that truly gives NMR core analysis its advantage over other core analysis techniques.

While ^{1}H is the best suited nucleus for core analysis, other NMR active nuclei show potential for unlocking more information for core analysis. The most obvious candidate nucleus for core analysis is ^{13}C. ^{13}C will be present in any oil contained within core samples. The downside of employing ^{13}C is its low natural abundance. Approximately, only 1% of naturally occurring carbon is ^{13}C. This leads to a lower signal-to-noise ratio (SNR) for the ^{13}C data leading to longer scan times as compared to ^{1}H. A second candidate nucleus for NMR core analysis is ^{23}Na. Like hydrogen, ^{23}Na has a natural abundance of nearly 100%. However, ^{23}Na will be dissolved in water in the brine present in core samples. Therefore, unlike ^{1}H which is present in 100% of both the water and oil molecules in a core sample, ^{23}Na will only be present to a reduced concentration in the brine (for example, 2% NaCl brine). This reduces the amount of ^{23}Na as compared to ^{1}H again leading to longer scan times.

Beyond the difference in abundance, the properties of the nuclei also lead to further reductions in sensitivity for ^{23}Na and ^{13}C as compared to ^{1}H. The NMR sensitivity is given by Equation 1

$$NMR\ Sensitivity \approx \gamma^3 B_0^2 N I(I+1) \qquad (1)$$

γ is the gyromagnetic ratio of the NMR active nuclei, B_0 is the strength of the magnetic field, N is the number of active nuclei per volume of sample and I is the nuclear spin (I = ½ for both ^{1}H and ^{13}C and I = 3/2 for ^{23}Na). From Equation 1, it is obvious that γ is the most important term in determining NMR sensitivity. For example, if a ^{13}C enriched sample existed with the same number of active nuclei per ml as ^{1}H and the NMR data were recorded at the same fixed field B_0 for each sample, the ratio of ^{1}H NMR sensitivity to ^{13}C sensitivity would be given by Equation 2

$$\frac{1H\ NMR\ senstivity}{13C\ NMR\ senstivity} = \frac{\gamma_H^3 B_0^2 N_H I(I+1)}{\gamma_C^3 B_0^2 N_C I(I+1)} = \frac{\gamma_H^3}{\gamma_C^3} \qquad (2)$$

The gyromagnetic ratios of ^{1}H, ^{13}C and ^{23}Na are 42.577 MHz/T, 10.75 MHz/T, and 11.26 MHz/T respectively [1]. This means that if all else is equal (B_0, N, I in equation 1) the NMR sensitivity of ^{1}H is still approximately 60 times higher than ^{13}C or ^{23}Na.

One way to reduce the difference in sensitivity due to the difference in gyromagnetic ratio is to employ a higher magnetic field for the ^{23}Na or ^{13}C measurements as compared to ^{1}H. For example, as shown in Equation 3, if a higher magnetic field is employed for ^{13}C measurements as compared to ^{1}H measurements then the ratio of NMR sensitivity will be reduced. Again, this is assuming an enriched ^{13}C sample is employed with the same number of ^{13}C per ml of sample as a corresponding ^{1}H sample.

$$\frac{1H\ NMR\ senstivity}{13C\ NMR\ senstivity} = \frac{\gamma_H^3 B_0^2 N_H I(I+1)}{\gamma_C^3 B_0^2 N_C I(I+1)} = \frac{\gamma_H^3 B_0^2}{\gamma_C^3 B_0^2} = \frac{(42.577 MHz/T)^3 (0.79T)^2}{(10.75\ MHz/T)^3 (3.14T)^2} = 3.93 \qquad (3)$$

Traditionally, low field ^{1}H NMR instruments (~0.05T) have been popular for use in petrophysics laboratories as they compare favorably, and reliably, to NMR logs done downhole in the field [2]. In addition, the lower field also reduces the issue of high magnetic susceptibility of core samples as compared to higher field instruments. However, higher field instruments present several distinct advantages for ^{1}H NMR measurements including faster scan times for a given signal-to-noise ratio (SNR), and superior detection of short relaxation elements due to their shift to longer relaxation times. For these reasons, higher field instruments have become more popular in recent years for use in ^{1}H NMR core analysis.

Recently, a new variable field magnet (MR Solutions, Guildford, Surrey, UK) has been introduced to NMR core analysis measurements. This work has been spearheaded by the Magnetic Resonance Imaging (MRI) centre at the University of New Brunswick (UNB). As outlined by Vashee et al. [3], this variable field magnet can be tuned to any field between approximately 0.01T and 3.1T. For core analysis experiments, the magnet was initially configured to work at 0.79 T and 3 T. These fields were chosen because

the same Larmor frequency (γB_0) can be produced for ^1H, ^{13}C and ^{23}Na (see Equations 4,5 and 6). The same Larmor frequency meant that the same RF coil can be employed for both excitation and detection for all three nuclei.

$$Larmor\ Frequency\ (1H) = \gamma B_0 = (42.577\text{MHz/T})(0.79\text{T}) = 33.64\ \text{MHz} \quad (4)$$

$$Larmor\ Frequency\ (13C) = \gamma B_0 = (10.75\text{MHz/T})(3.14\text{T}) = 33.63\ \text{MHz} \quad (5)$$

$$Larmor\ Frequency\ (23Na) = \gamma B_0 = (11.26\text{MHz/T})(2.99\text{T}) = 33.69\ \text{MHz} \quad (6)$$

Using this variable field magnet, the UNB MRI centre has completed several studies looking at how a combination of ^1H and ^{13}C NMR measurements can be employed to evaluate the wettability in supercritical CO_2-brine-rock interactions [4] as well as for fluid quantification and kerogen assessment in shales [5]. In addition, the MRI centre has looked at employing ^{13}C NMR measurements to characterize signal density and relaxation times of crude oils [6] along with the wettability of core samples [7]. Finally, it was shown that direct hydrocarbon imaging in porous media could be completed with ^{13}C [8,9].

Perhaps the most important core analysis measurement for which a multinuclear NMR measurement is well suited is determining the relative concentration of oil and water in a core sample. Traditional saturation determination methods such as the Dean-Stark Method employs the use of both heat and solvents, both of which can alter the sample and are destructive [10]. Another method for determining the relative concentration of oil and water in a core sample is to employ a micro-CT measurement. In these measurements, it is common practice to add sodium iodide (NaI) to brine during laboratory flooding experiments. The presence of iodine helps increase the contrast between oil and water for in-situ saturation monitoring using micro-CT. In recent years however, researchers at TotalEnergies have shown [11,12] that the presence of NaI can alter the wettability of the sample under observation and this alteration can lead to a bias in SCAL experiments.

Nuclear Magnetic Resonance (NMR) should be well suited to determine the relative oil/water concentration as it is a non-invasive technique which has been employed for years in laboratories to determine the total fluid content in core samples. As outlined earlier, the active nucleus in traditional NMR core analysis has been hydrogen (^1H). It can be difficult for ^1H NMR to distinguish between oil and water as ^1H is present in both fluids. Employing ^1H NMR to distinguish between oil and water requires the use of either doping agents to shorten the relaxation time of water as compared to oil, specialized pulse sequence such as T_1-T_2 maps or employing D_2O based brines in lieu of H_2O. All these methods can be time consuming, expensive and/or non-conclusive.

On the other hand, a multinuclear NMR measurement could be employed to distinguish between oil and water in a core sample. A ^1H measurement would yield the total fluid content of a core sample saturated with both oil and water. While a ^{13}C measurement would yield the oil concentration independently. Conversely a ^{23}Na measurement would yield the water concentration independently. A multinuclear NMR measurement of oil and water concentration could become an important tool in core analysis. The UNB MRI centre has completed a recent study [13,14], where the relative concentration of water and oil in porous media was determined using ^{13}C and ^1H magnetic resonance measurements. They also successfully confirmed the validity of the saturation derived from NMR by comparing it to the saturations derived from the Dean-Stark technique.

Inspired by the work from the University of New Brunswick, we have developped a new NMR probe capable of observing both ^{13}C and ^{23}Na at lower field. As will be outlined in this paper, this has involved overcoming a whole series of experimental challenges including the low natural abundance of ^{13}C, background signal from Teflon and electrical noise as well as working at a lower magnetic field as compared to UNB. The paper is meant to be status report on our progress to date on development of this low field ^{13}C and ^{23}Na NMR probe.

2 Probe Design and Sensitivity Estimates

It was decided that the best approach for the design of the new $^{13}C/^{23}Na$ NMR probe would be to build it as a new probe for our existing 0.3T magnet. This magnet is built by Oxford Instruments (Oxford Instruments, High Wycombe, UK) and is designed for ^1H NMR experiments at a Larmor frequency of 12.9 MHz and can accept different probes to handle samples of different sizes. The new probe was designed to be a dual tune probe capable of tuning to the Larmor frequencies of both ^{13}C (3.25 MHz) and ^{23}Na (3.41 MHz) and will accept samples 1.5” in diameter and 2” in length.

The Larmor frequencies for ^{13}C and ^{23}Na provided by this probe will be approximately ten times lower than that employed by UNB. In addition, whereas all of UNB’s measurements (^1H, ^{13}C and ^{23}Na) were done with the same Larmor frequency (~33 MHz see Equations 4,5 and 6), the measurements done with the new probe will be done at the same magnetic field (0.3T) but differing Larmor frequencies. This begs the question, what will the relative

sensitivity of each NMR measurement with each nuclei for this probe? Employing Equation 1, the relative sensitivity of NMR measurements of ^{1}H in water vs ^{13}C in decane vs ^{23}Na in 10% NaCl brine can be calculated. Table 1 summarizes the results where the sensitivities are scaled to ^{13}C in decane which is assigned a value of 1.

Table 1. Relative sensitivity of ^{1}H in water vs ^{13}C in decane vs ^{23}Na in 10% NaCl brine.

Nuclei	Bulk Sample	Relative Sensitivity
^{13}C	Decane	1
^{1}H	Water	13400
^{23}Na	10% NaCl Brine	12.8

3 Initial Probe Testing and Diagnosing Noise Problems

Clearly, observation of ^{13}C and ^{23}Na will be a challenge with this new probe but the interest overcame the difficulty and a probe was built, and testing began. Initial tests showed that the noise level of the probe was higher as compared to the ^{1}H probe. This noise was fast decaying and would manifest itself in T_2 distributions as a short T_2 signal that could easily be interpreted as coming from fluid in small pores of a core sample. The first step in investigating the noise was to look at the free induction decay (FID) of the empty ^{13}C probe inside and outside the magnet. The upper two panels of Figure 1 (labeled as A and B) show the result of this survey. The upper right-hand panel (B) shows the FID when the cell is outside the magnet while the upper left-hand panel shows the FID when the cell is inside the magnet (A). Comparing these two decays clearly shows that the fast-decaying noise is only occurring when the probe is in the magnet and therefore must be caused by the presence of the magnetic field. The fact that the noise does not appear outside the magnet indicates that it is not simple electronic noise.

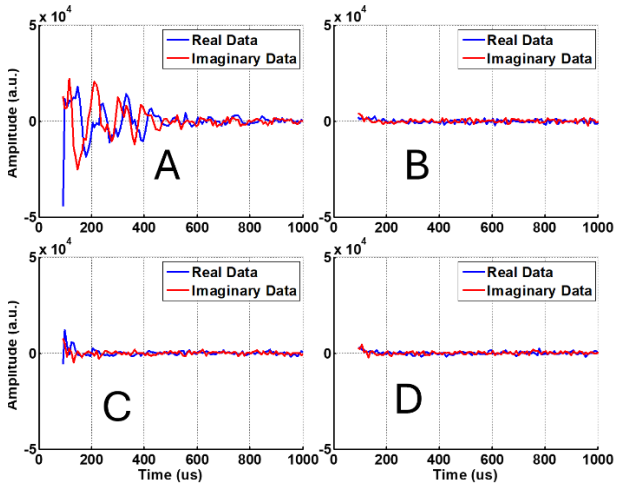

Fig. 1. Free induction decays of ^{13}C probe inside and outside the magnet. The upper right-hand panel (labeled as B) shows the FID when the cell is outside the magnet while the upper left-hand panel (labeled as A) shows the FID when the cell is inside the magnet. Comparing these two decays clearly shows that the fast-decaying noise is only occurring when the probe is in the magnet. The lower panels show the free induction decay measurements inside (labeled as C) and outside the magnet (labeled as D) following the application of copper shielding.

Because the noise only occurs when the probe is in the magnet, it was determined that acoustic waves created in the frame of the probe caused by the pulsed RF field was the source of the observed noise. The body of our probe was made of aluminum which is very susceptible to acoustic ringing and dropping the Larmor frequency from 12.9 MHz for ^{1}H to 3.24 MHz for ^{13}C further accentuated the problem. According to Buess and Petersen [15] acoustic ringing can be limited in NMR probes by employing copper shielding. The inner surfaces of the probe were then coated with copper and the inside and outside the magnet FID measurements were repeated. The lower panels of Figure 1 show the results of these measurements. Comparing the lower-right panel to the lower-left panel shows the difference copper shielding made to the fast-decaying noise present when the probe is in the magnet. While the noise level has been reduced, the noise level with copper shielding when the probe is in the magnet is still not as low as when the probe is out of the magnet.

While the reduction in noise did allow some data to be recorded with longer tau values, it still posed a problem for data acquisition of samples with low levels of signal (^{13}C samples in particular). Therefore, further experiments were conducted assessing the origin of the persistent fast decay

noise. These efforts included replacing the aluminum frame with a plastic one with the thought that the noise was persistent acoustic ringing which could not be eliminated by copper shielding alone. Unfortunately, the noise signal persisted and was present no matter what sample was tested (including if no sample was present in the probe). The blue trace in Figure 2 shows a T_2 distribution recorded with an empty probe. Clearly signal continues to be present when none should be. Eventually, it was determined that the signal originated from ^{13}C present in the Teflon tube around which the RF coil in the probe is wrapped. The red trace in Figure 2 shows the T_2 distribution when 184g of Teflon are inserted into the probe. Teflon is traditionally chosen as the material for RF coil holders for ^{1}H probes because Teflon is hydrogen free. However, Teflon is not carbon free and was not a good choice to hold the RF coil in the ^{13}C probe. To eliminate the signal from carbon, the Teflon RF coil holder needed to be replaced. Several alternate materials were tested and eventually the Teflon RF coil holder was replaced with one made from ceramic which was free of both carbon and hydrogen.

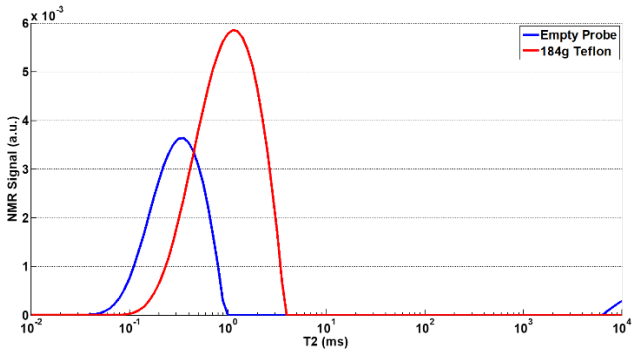

Fig. 2. T_2 distribution of empty probe (blue trace) vs Teflon (red trace). NMR signal is present with empty probe indicating that something in the body of the probe has ^{13}C. It was determined that the signal originated from ^{13}C present in the Teflon tube around which the RF coil in the probe is wrapped. The red trace shows the T_2 distribution when 184g of Teflon are inserted into the probe. It overlaps with the signal from the empty probe confirming that the empty probe background signal is originating from Teflon.

4 ^{23}Na Probe Tuning, Calibration and Initial Bulk Fluid Measurements.

4.1 Initial Bulk Fluid Measurements And Estimation of Scan Times

The first step in the commissioning of the ^{23}Na probe was to tune and calibrate the probe. A sample of 25% solution of NaCl dissolved in water was employed as a calibration standard. 90 ml (107.3g) of this calibration fluid was put in the magnet which corresponds to 26.78 g of NaCl in the calibration sample. Then using the molar masses of NaCl (58.44 g/mol) and Na (22.99 g/mol), it can be calculated that 10.53 g of ^{23}Na were present in the calibration sample. This value was used to calibrate the machine units to g of Na observed and the calibration constants shown in the first column of Table 2 were derived for ^{23}Na.

Table 2. Calibration constants for ^{13}C and ^{23}Na probes.

Probe	^{23}Na	^{13}C
Frequency (MHz)	3.41	3.25
P90 (µs)	44.19	34.87
P180 (µs)	88.72	69.75
Calibration Fluid	25% NaCl Brine	Glycerol

Once the probe was tuned and calibrated, the first series of measurements was to observe the amount of ^{23}Na in different NaCl brines of varying concentrations (for each sample approximately 100g of brine were measured). Figure 3 shows the T_2 distributions of NaCl brine of four different concentrations (2%, 5%, 10% and 25%). The T_2 distributions were recorded using a Carr-Purcell-Meiboom-Gill (CPMG) pulse sequence [16]. Table 3 summarizes all the data recorded. The agreement between the expected and NMR observed ^{23}Na mass was good. Any bias observed in comparing the expected and observed masses could be improved with more care and experience when calibrating with ^{23}Na brine.

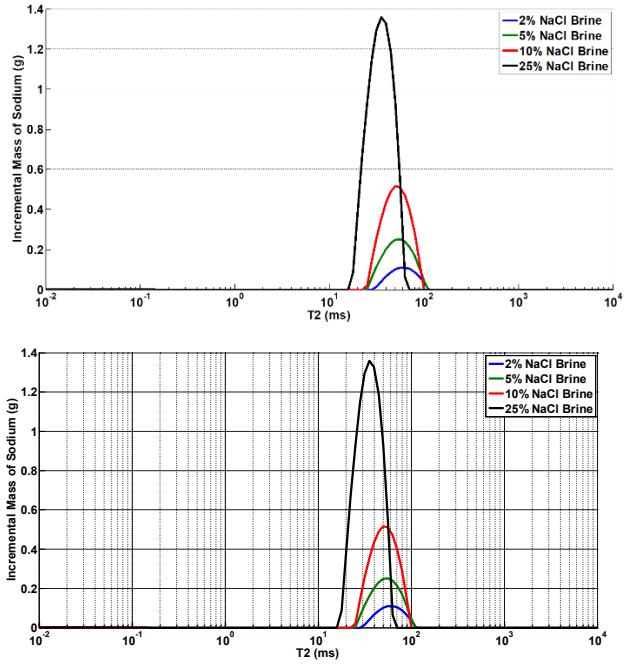

Fig. 3. T_2 distributions of bulk NaCl brines (~100 g) of different concentrations. Each distribution was recorded with a CPMG pulse sequence with a 129 µs tau, 1250 echoes and a recycle delay of 750 ms. The scan time and SNR of each T_2 distribution are summarized in Table 3.

Table 3. Data derived from T_2 distributions shown in Figure 3 of bulk NaCl brines of different concentrations.

Brine Conc.	Brine Mass	Expected ^{23}Na Mass (based on Molar masses)	NMR obs. ^{23}Na Mass	SNR	Scan Time
2%	100g	0.787g	0.827g	200.02	53m 24s
5%	100.3g	1.973g	2.062g	106.39	2m 25s
10%	98.8g	3.890g	3.989g	151.85	1m 22s
25%	100.8g	9.910g	10.018g	356.62	1m 23s

According to the data summarized in Table 3, the T_2 distribution of a 98.8g of 10% NaCl brine was scanned to a signal-to-noise ratio of 151.85 in 82 seconds. This value can now be used to derive how long it will take to scan a 1.5" diameter and 2" long core sample with a porosity of 10 p.u. half saturated with oil and half saturated with 10% NaCl brine to the same SNR. This would be considered a typical measurement for determining the relative concentration of oil and water in a core sample via a combination of ^{1}H and ^{23}Na NMR measurement. This calculation is outlined below.

1) Calculate volume of 98.8g of 10% NaCl using density of 1 cm^3/1.07 g

$$100g\ of\ 10\%\ NaCl\ Brine \rightarrow 98.8g\ x\ \frac{1cm^3}{1.07g} = 92.33\ cm^3$$

2) Determine bulk volume, pore volume and volume of NaCl brine in a 1.5" (3.81 cm) diameter, 2" (5.08 cm) long, 10% porosity core sample.

$$Bulk\ Volume = \pi\left(\frac{3.81cm^3}{2}\right)^2 (5.08cm) = 57.92cm^3$$

$$Pore\ Volume = Porosity x Bulk\ Volume = (0.1)(57.92cm^3) = 5.79cm^3$$

$$Volume\ of\ NaCl\ in\ Core = \frac{5.79cm^3}{2} = 2.90cm^3$$

3) Determine the time it will take to scan the core sample to the same SNR as 98.8g of 10% NaCl brine employing the fact that SNR is proportional to sample volume x $\sqrt{measurment\ time}$.

$$SNR\ (98.8g\ NaCl\ brine) = SNR\ (Volume\ of\ NaCl\ brine\ in\ core)$$

$$Vol(98.8g\ NaCl\ Brine)\sqrt{Meas.time\ 100g\ NaCl\ Brine} = Vol(NaCl\ in\ core)\sqrt{Meas.time\ NaCl\ brine\ in\ core}$$

$$(92.3\ cm^3)\sqrt{82s} = (2.9cm^3)\sqrt{Meas.time\ NaCl\ Brine\ in\ core}$$

$$Meas.time\ NaCl\ in\ core = 83066\ s = 23\ hrs$$

The scan time could be further reduced by scanning the sample to a lower SNR. In a previous investigation [17], it was shown that an SNR of 80 is adequate to accurately determine T_2 based pore size distributions and porosity. Scanning to an SNR of 80 in lieu of 151.85 would further reduce the scan time by a factor of 0.277 ((80/151.85)^2) reducing the measurement time to 6.4 hrs. While 6.4 hrs for the ^{23}Na measurement may seem like a lengthy measurement time especially when compared to the short measurement times associated with ^{1}H NMR, it should be remembered that the relative oil/water saturation measurement is typically done via a Dean-Stark measurement which is both destructive to the sample and can take days to complete.

4.2 Other Bulk Measurements With ^{23}Na Probe.

Beyond the T_2 measurements, other test measurements continued with the bulk NaCl samples. Figure 4 shows the saturation profile recorded with the ^{23}Na probe and a 10% NaCl bulk brine sample. The profile was recorded using a spin echo single point imaging (SE-SPI) pulse sequence [18]. Figure 5 shows the T_1 distribution recorded with the 10% NaCl bulk brine sample. Finally, Figure 6 shows the results of a diffusion measurement (stimulated echo pulse gradient pulse [19]) recorded for ^{23}Na inside the 10% (1.9M) NaCl bulk brine sample. From the diffusion fit (Figure 6) the diffusion measurement took 16 hours to complete and the diffusion constant derived from the data was 1.96E-9 m^2/s. This is consistent with the known value the diffusion constant of Na in a 2M NaCl sample (1.82E-9 m^2/s [20]). .

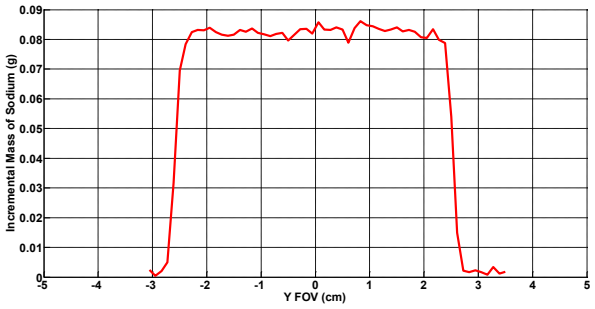

Fig. 4. SE-SPI saturation profile recorded with the Na probe and a 10% NaCl bulk brine sample (98.8 g). The resolution of the scan was 64 for a field of view of 7cm. The scan time was 3 minutes and 14 seconds to an SNR of 209.07.

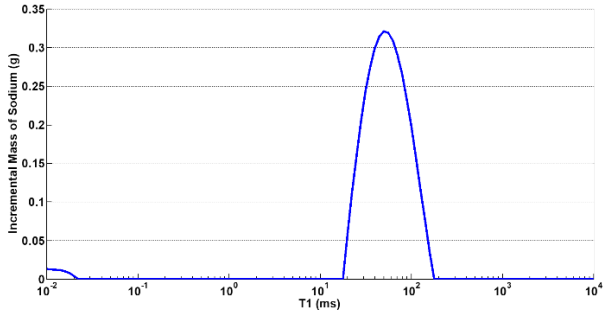

Fig. 5. T_1 distribution recorded with a 10% NaCl bulk brine sample (98.8g). The scan time was 65 minutes to an SNR of 213.74.

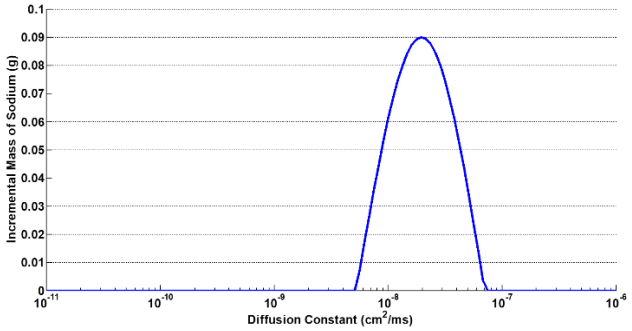

Fig. 6. Results of diffusion measurement completed on 10% NaCl bulk brine sample (98.8g). . The scan time was 15 hours and 37 minutes to an SNR of 200.2.

4 ^{13}C Probe Tuning, Calibration and Initial Bulk Fluid Measurements.

As with the ^{23}Na probe, the first step in the commissioning of the ^{13}C probe was to tune and calibrate the probe. However, unlike ^{23}Na, the choice of calibration fluid was not so straight forward. Initially, decane was chosen as a calibration fluid. However, it quickly became apparent that the T_2 relaxation time of bulk decane (~4000 ms) was too long to calibrate the probe quickly. A new calibration fluid for the ^{13}C probe needed to be selected. Ideally, the T_2 distribution of this fluid should be scanned to a higher SNR in a shorter period of time as compared to decane. Eventually, glycerol was chosen as calibration fluid. While glycerol has a lower number of moles of ^{13}C per ml (0.410 mmoles/ml) as compared to decane (0.513 mmoles/ml) it has much shorter T_2 relaxation which means more NMR measurements can be repeated and averaged per unit of time leading to an increase in SNR. Figure 7 shows the T_2 distribution recorded with the ^{13}C probe for a 100g bulk sample of glycerol. The T_2 relaxation time of bulk glycerol is approximately 40 ms. This meant that it could be scanned to the same SNR as decane in approximately 1/100th the time. For example, for the T_2 distribution of glycerol shown in Figure 7, a signal-to-noise ratio of 12.59 was achieved 82s.

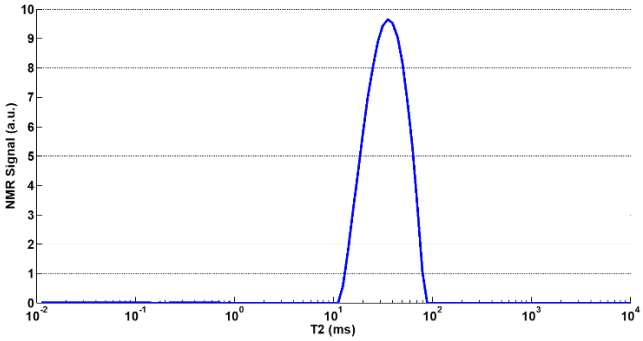

Fig. 7. T_2 distribution for 100g of bulk glycerol. The distribution was recorded with a CPMG pulse sequence with a 200 µs tau, 1250 echoes and a recycle delay of 750 ms. The scan time was 82 seconds to an SNR of 12.59.

After completion of the T_2 calibration measurements with glycerol, a saturation profile was also completed on a 115g bulk glycerol sample employing a spin echo single point imaging (SE-SPI) pulse sequence. Figure 8 shows the results of this measurement.

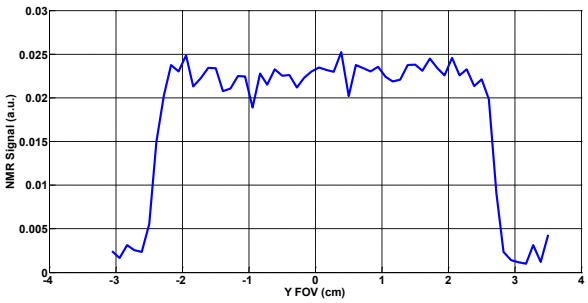

Fig. 8. Saturation profile recorded with an SE-SPI pulse sequence with the ^{13}C probe and a 115g bulk sample of glycerol. The resolution of the scan was 64 for a field of view of 7cm. The scan time was 37 minutes and 46 seconds to an SNR of 50.29.

5 Proof of principal relative concentration measurement using bulk samples and ^{13}C probe.

As mentioned earlier in this paper, perhaps the most important core analysis measurement for which a multinuclear NMR measurement is well suited is determining the relative concentration of oil and water in a core sample. As a first test of the capability of this ^{13}C probe to complete this measurement, an experiment was conducted with bulk oil and water samples. The object of this experiment was to prove that the ^{13}C probe would only observe the signal from oil and not water. The experiment was then repeated with the ^{1}H probe to show that this probe would observe both water and oil. To complete the experiments, two distinct samples were employed (Figure 9 – Right Hand Panel). Each sample contained the same amount of glycerol (25.5ml – NMR volume) stacked on top of either an empty sample (Sample 1) or a sample filled with water (Sample 2 - 5.5 ml - NMR volume). Measurements with Sample 1, both the ^{1}H probe and the ^{13}C probe should show the same result (i.e. only signal from the glycerol which has both hydrogen and carbon). On the other hand, any data recorded with Sample 2 should show signal from both water and glycerol when the ^{1}H probe is employed. While a measurement of Sample 2 with the ^{13}C probe should only show glycerol and as a result a scan of either sample should look the same. The left hand panel of Figure 9 shows the result of the saturation profile measurement of Samples 1 and 2 with the ^{1}H and ^{13}C probes. The upper two plots show the saturation profiles measured with Samples 1 and 2 with the ^{13}C probe. Each plot shows the same profile (only from glycerol). As expected, there is no signal from the water sample when Sample 2 is measured. The lower two plots of Figure 9 show the saturation profiles recorded with the ^{1}H probe. The lower left panel shows the profile recorded with Sample 1 and shows only glycerol as glycerol is the only species present. The lower right panel of Figure 9 shows the profiles of both water and glycerol.

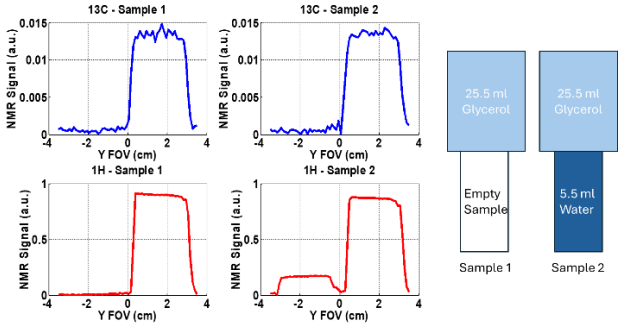

Fig. 9. Saturation profiles acquired with ^{1}H and ^{13}C probes of Samples 1 and 2 (Right Hand Panel). The upper two plots show the saturation profiles measured with Samples 1 and 2 with the ^{13}C probe. Each plot shows the same profile (only signal from glycerol). There is no signal from the water sample when Sample 2 is measured. The lower two plots show the saturation profiles recorded with the ^{1}H probe. The lower left panel shows the profile recorded with Sample 1 and shows only glycerol as glycerol is the only species present. The lower right panel shows the profile recorded with Sample 2 shows the profiles of both water and glycerol.

Figure 10 shows the T_2 distributions recorded with Samples 1 and 2 with both the ^{13}C and ^{1}H probes. As expected, the T_2 distributions recorded with the ^{13}C probe (black and green traces) show only one peak from glycerol. For the T_2 distributions recorded with the ^{1}H probe, the distribution recorded with Sample 1 (red trace) shows just one peak while the distribution recorded with Sample 2 shows two peaks (blue trace). The peak with the shorter T_2 value recorded with the ^{1}H probe for Sample 2 (blue trace) is attributed to glycerol while the longer T_2 peak is water. Finally, it should be noted that for all the plots shown in Figure 10, the area under the glycerol peaks have been scaled to match the volume of the glycerol peak recorded with the ^{1}H probe with Sample 1. Using this scaling method, ensures that the lower signal-to-noise ratio ^{13}C data is properly calibrated with the higher SNR ^{1}H data.

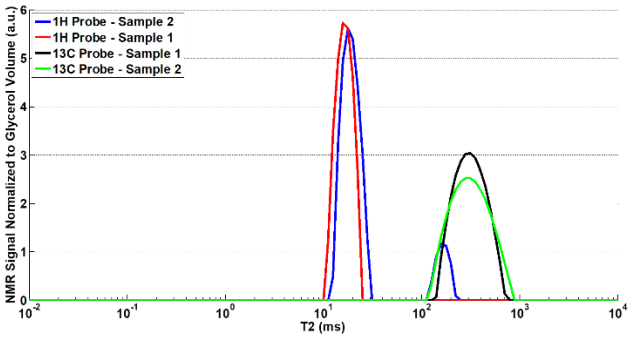

Fig. 10. T_2 distributions recorded with ^{1}H and ^{13}C probes for Samples 1 and 2 with both the ^{13}C and ^{1}H probes. The T_2 distributions recorded with the ^{13}C probe (black and green traces) show only one peak from glycerol. The distribution recorded with Sample 1 (red trace) with the ^{1}H probe shows just one peak while the distribution recorded with Sample 2 shows two peaks (blue trace). The peak with the shorter T_2 value recorded with the ^{1}H probe for Sample 2 (blue trace) is attributed to glycerol while the longer T_2 peak is water.

6 Preliminary ^{13}C measurements of a saturated core sample.

Having commissioned and calibrated the ^{13}C probe as well as having shown that an oil/water relative concentration measurement is feasible with the probe, it was decided to attempt to measure ^{13}C signal from a saturated core sample. A 1.5" diameter, 2" long sandstone sample with a pore volume of approximately 8 ml was 100% saturated with decane. The blue trace in Figure 11 shows the T_2 distribution recorded with the ^{1}H probe for this saturated sample. The observed pore volume for this sample was 7.75 ml and was scanned to an SNR of 3129 in 1 minute and 40

seconds. The red trace in Figure 11 shows the T_2 distribution recorded with the ^{13}C probe for this saturated sample. This distribution was measured to an SNR of 7.34 in 30 hours. It should be noted that the area under the T_2 distribution recorded with the ^{13}C probe was normalized to the pore volume of the sample as derived from the ^{1}H data. This was necessary as the ^{13}C probe was not calibrated with decane prior to the measurement. The ^{1}H and ^{13}C T_2 distributions shown in Figure 11 appear very similar which gives confidence that the T_2 distribution recorded with the ^{13}C probe originates from decane in the core sample despite the low SNR. Finally, the small signal seen at long T_2 (~2500 ms) for the ^{13}C data (Figure 11 – red trace) is due to a small amount of bulk decane which has accumulated

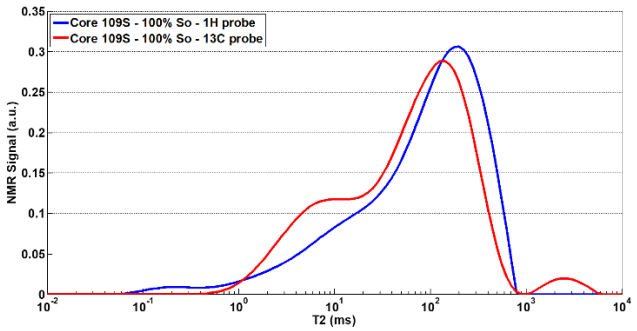

Fig. 11. T_2 distributions recorded with ^{1}H and ^{13}C probes for the same sandstone sample 100% saturated with decane. For the ^{1}H probe (blue trace), the distribution was recorded with a CPMG pulse sequence with a 50 µs tau and a recycle delay of 3750 ms. The scan time was 1 minute and 40 seconds to an SNR of 3129. For the ^{13}C probe (red trace), the distribution was recorded with a CPMG pulse sequence with a 1000 µs tau and a recycle delay of 7500 ms. The scan time was 30 hours to an SNR of 7.34. The small signal seen at long T_2 (~2500 ms) for the ^{13}C data (red trace) is due to a small amount of bulk decane which has accumulated at the bottom of the core holder in the magnet.

Unfortunately, the SNR was lower than expected for this measurement of the 100% decane saturated core sample with the ^{13}C probe. This decrease in SNR was attributed to all the iterations the probe has undergone throughout this testing process to address problems with the design. For example, the original RF coil holder was made of Teflon and was replaced with one made of ceramic to avoid background signal from the ^{13}C in the Teflon. This replacement meant that both the RF coil holder and RF coil were replaced. This replacement did not involve optimization of the tune circuit to match the new RF coil. Figure 12 shows the tuning trace of the transmit circuit for the current iteration of the ^{13}C probe with a ceramic RF coil holder. Clearly, the circuit is not optimized as the minimum (bottom of "V" shape) in the transmitted RF energy should correspond with the resonance frequency of the probe. There is room for improvement in the probe design which will lead to a better SNR performance.

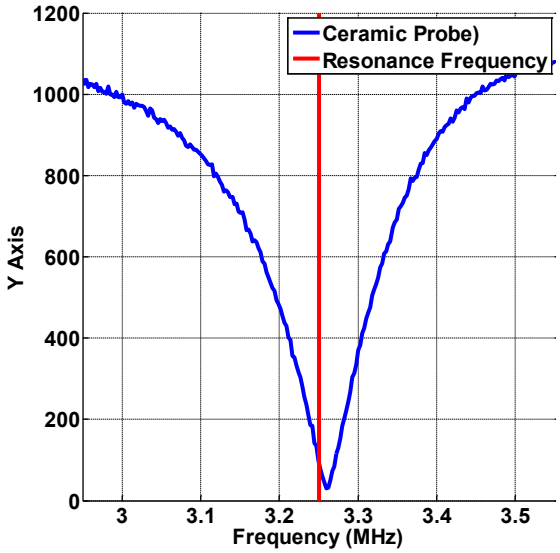

Fig. 12. The tuning trace of the transmit circuit for the current iteration of the ^{13}C probe with a ceramic RF coil holder is shown (blue trace). Clearly, the circuit is not optimized as the valley in the transmitted RF energy should correspond with the resonance frequency of the probe (red trace).

7 Conclusions.

A new dual tune ^{13}C and ^{23} Na NMR probe has been developed. This probe works with an existing 0.3T magnet and provides a Larmor frequency of 3.24 MHz for ^{13}C and 3.42 MHz for ^{23}Na. For ^{23}Na, the probe has been successfully commissioned and calibrated employing a 25% NaCl brine in water as a calibration fluid. Several different concentrations (2%, 5%, 10% and 25%) of NaCl brine were then probed to determine the scan time and SNR for each. For example, it was determined that it takes the ^{23}Na probe two minutes and twenty-five seconds to scan a T_2 distribution of 92.33 ml of a 10% NaCl brine to an SNR of 151. This information was then used to estimate the scan time required to record the relative brine saturation of a core sample (pore volume = 5.8ml) fifty percent saturated with brine. Beyond T_2 measurements, T_1 and SE-SPI saturation profile measurements of the 10% NaCl brine were also recorded with the ^{23}Na probe.

The ^{13}C probe was also successfully commissioned and calibrated. The calibration fluid employed for this probe was glycerol. It was shown that the T_2 distribution of 100g of glycerol can be measured to a signal-to-noise ratio of 12.59 in 82s. In addition, a proof of principal measurement with bulk water and glycerol samples along with our ^{1}H and ^{13}C probes was completed. This showed that a multi-nuclear NMR based oil/water relative saturation measurement is feasible.

Finally, the T_2 distribution of a core sample 100% saturated with decane was recorded with the ^{13}C probe. The T_2

distribution matched corresponding distribution recorded with the ^{1}H probe. Unfortunately, the SNR was very low for this measurement with the ^{13}C probe. While the SNR for ^{13}C measurements is expected to be low due to the low natural abundance of ^{13}C, the SNR of this measurement of the 100% saturated core sample was lower than expected and hence the scan time longer than expected. This was attributed to a decrease in the quality of the tune of the transmit and receive circuits of the probe. As mentioned in the introduction, this paper is meant to be a status report on our progress to date on development of this low field ^{13}C and ^{23}Na NMR probe. There has obviously been success this year in the development, but future work is needed. The next steps will be to build a second version of the probe addressing all the challenges identified in our current probe design. Specifically, the resistance and capacitance of the resonant circuit in the new probe will be optimized to better match the resonance frequency of ^{13}C and maximize the signal-to-noise ratio. This should mean that the results reported in this paper are a worse case scenario and future ^{13}C and ^{23}Na data recorded with future versions of the probe will yield better SNR data with shorter scan times.

References

1. Nishimura, D.G., *Principles of Magnetic Resonance Imaging*. Ed. 1.1. (2010).
2. Coates, G.R., Xiao, L., and Prammer, M.G., *NMR Logging. Principles & Applications*, (1999).
3. Vashaee, S., Li, M., MacMillan, B., Enjilela, R., Green, D., Marcia, F., and Balcom, B.J. "Magnetic Resonance Imaging with a Variable Field Superconducting Magnet that can be Rotated for Vertical or Horizontal Operation", *International Symposium of the Society of Core Analysts, Vienna, Austria*, (12 pages), (2017).
4. Li, M., Kortunov, P., Lee, A., Marica, F., and Balcom, B.J. "Sandstone Wettability in Supercritical CO_2-Brine-Rock Interactions Evaluated with ^{13}C and ^{1}H Magnetic Resonance", *Chemical Engineering Journal,* **500**, 157100 (16 pages), (2024).
5. Zamiri, M.S., Ansaribaranghar, N., Aguilera, A.R., Marica, F., and Balcom, B.J. "Fluid Quantification and Kerogen Assessment in Shales Using ^{13}C and ^{1}H Magnetic Resonance", *International Symposium of the Society of Core Analysts, Fredericton, Canada,* (6 pages), (2024).
6. Ansaribaranghar, N., Zamiri, M.S., Romero-Zerón, L., Marica, F., Aguilera, A.R., Dick, M., Green, D., Nicot, B., and Balcom, B.J."^{13}C Magnetic Resonance Signal Density and Relaxation Times of Crude Oils", *International Symposium of the Society of Core Analysts, Fredericton, Canada*, (9 pages), (2024).
7. Ansaribaranghar, N., Zamiri, M.S., Pairoys, F., Fernandes, V., Romero-Zerón, L., Marica, F., Aguilera, A.R., Green, D., Nicot, B., and Balcom, B.J. "Characterizing Wettability Using ^{13}C Magnetic Resonance Relaxation Times ", *International Symposium of the Society of Core Analysts, Fredericton, Canada,* (11 pages), (2024).
8. Ansaribaranghar, N., Zamiri, M.S., Romero-Zerón, L., Marica, F., Aguilera, A.R., Green, D., Nicot, B., and Balcom, B.J."Direct Hydrocarbon Saturation Imaging in Porous Media with ^{13}C", *International Symposium of the Society of Core Analysts, Abu Dhabi, UAE*, (9 pages), (2023).
9. Ansaribaranghar, N., Zamiri, M.S., Romero-Zerón, L., Marica, F., Aguilera, A.R., Green, D., Nicot, B., and Balcom, B.J. "Direct Hydrocarbon Saturation Imaging in Porous Media with ^{13}C Magnetic Resonance", *Petrophysics* **66(1)**, 169-182, (2025).
10. McPhee, Colin, Reed, Jules and Zubizarreta, Izaskun. *Core Analysis: A Best Practice Guide*. Developments in Petroleum Science **Vol. 64**, Elsevier Science, (2015).
11. Pairoys, F., Caubit, C., Rochereau, L., Nepesov, A., Danielczick, Q., Agenet, N. and Nono, F., "Impact of Dopants on SCAL Experiments, Phase I", *International Symposium of the Society of Core Analysts, Abu Dhabi, UAE*, (9 pages), (2023).
12. Nono, F., Faisal, T.F., Fischer, F., Parioys, F., Regaieg, M., and Caubit, C., "Pore scale investigation of dopants and impact on wettability alteration", *International Symposium of the Society of Core Analysts, Fredericton, Canada* (9 pages), (2024).
13. Ansaribaranghar, N., Zamiri, M.S., Romero-Zerón, L., Marica, F., Aguilera, A.R., Green, D., Nicot, B., and Balcom, B.J. "Bulk Saturation Measurement of Water and Oil in Porous Media Using ^{13}C and ^{1}H Magnetic Resonance", *International Symposium of the Society of Core Analysts, Abu Dhabi, UAE*, (8 pages), (2023).
14. Ansaribaranghar, N., Zamiri, M.S., Romero-Zerón, L., Marica, F., Aguilera, A.R., Green, D., Nicot, B., and Balcom, B.J. "Bulk Saturation Measurement of Water and Oil in Porous Media Using ^{13}C and ^{1}H Magnetic Resonance", *Petrophysics* **66(1)**, 155-168, (2025).
15. Buess, M.L., Petersen, G.L., "Acoustic ringing effects in pulsed nuclear magnetic resonance probes", *Rev. Sci. Instrum.* **49**, 1151–1155 (1978)
16. Meiboom, S. and Gill, D., "Modified Spin-Echo Method for Measuring Nuclear Relaxation Times", Review of Scientific Instruments, **29**, 688-691, (1958).
17. Dick, M., Veselinovic, D., and Green, D., " The effect of SNR on T_2 distributions and T_1-T_2 Maps ", *International Symposium of the Society of Core Analysts, Fredericton, Canada* (2024).
18. Li L, Han, H. and Balcom, B., "Spin echo SPI methods for quantitative analysis of fluids in porous media"

methane storage capacity in organic-rich shales," *J. of Magn. Reson.*, **198**, 252-260, (2009).

19. Leu G, Fordham EJ, Hürlimann MD, Frulla P. "Fixed and pulsed gradient diffusion methods in low-field core analysis". *Magn Reson Imaging*. **23(2)** 305-9. (2005).